Chapter 5
Semi-active Inerter and Adaptive Tuned Vibration Absorber

Abstract This chapter presents a novel framework to realize the semi-active inerter, and proposes a novel semi-active-inerter-based adaptive tuned vibration absorber (SIATVA). The proposed semi-active inerter can be realized by replacing the fixed-inertia flywheel in the existing flywheel-based inerters with a controllable-inertia flywheel (CIF). Then, by using the proposed semi-active inerter, a SIATVA is constructed, and two control methods, that is the frequency-tracker-based (FT) control and the phase-detector-based (PD) control, are derived. The experimental results show that both the FT control and the PD control can effectively neutralize the vibration of the primary mass, although the excitation frequency may vary. The proposed SIATVA can also tolerate the parameter variation of the primary system. As a result, it can be applied to a variety of primary systems without resetting the parameters. The performance degradation by the inherent damping is also demonstrated.

Keywords Semi-active inerter · Adaptive tuned vibration absorber · Controllable-inertia flywheel · Physical embodiments · Experiments

5.1 Introduction

To date, three types of inerters have been proposed, including the rack-pinion inerter (Smith 2002; Chen et al. 2009), the ball-screw inerter (Wang and Su 2008; Chen et al. 2009) and the hydraulic (or fluid) inerter (Wang et al. 2011; Gartner and Smith 2011; Tuluie 2010). See Chap. 1 for details. Note that for the rack-pinion inerters (Smith 2002; Chen et al. 2009), the ball-screw inerter in Wang and Su (2008), Chen et al. (2009), and the hydraulic inerters in Wang et al. (2011), Gartner and Smith Tuluie (2011), Tuluie (2010), the inertance cannot be adjusted online. This means the inertance cannot be adapted according to the variation of the external disturbances and environmental conditions.

To make the inertance adjustable, in Tsai and Huang (2011), a variable-inertia device (VID) by using a magnetic planetary gearbox is proposed. The variable-inertance inerter is actually a semi-active device, similar to the semi-active dampers and semi-active springs, where parameters (inertance, damping coefficient, and

M. Z. Q. Chen and Y. Hu, *Inerter and Its Application in Vibration Control Systems*, https://doi.org/10.1007/978-981-10-7089-1_5

spring stiffness) can be adjusted online by consuming small amount of energy. From this point of view, we proposed the semi-active inerter concept in Chen et al. (2014), which is defined as the inerter whose inertance can be controlled online. Almost at the same time, other terminologies regarding variable-inertance inerter were independently proposed, such as the "adaptive inerter" in Li et al. (2014), Li et al. (2015), "inerter which enables changes of inertance" (Brzeski et al. 2015). In this chapter, we uniformly use the term "semi-active inerter" to represent the inerter whose inertance can be adjusted online. Moreover, note that the term "semi-active inerter" was first used in Zhang et al. (2010). However, the so-called semi-active inerter in Zhang et al. (2010) is not a variable-inertance inerter as defined in Chen et al. (2014) and this chapter, but a semi-active suspension with a passive inerter.

In terms of the physical embodiments of semi-active inerter, in Hu et al. (2017), we proposed a general framework to realize the semi-active inerter, that is the inertance can be controlled online by adjusting either the transmission ratio or the moment of inertia of the flywheel. From this point of view, the variable-inertia device in Tsai and Huang (2011) and the "inerter which enables changes of inertance" in Brzeski et al. (2015) are realized by adjusting the transmission ratio based on a magnetic planetary gearbox and a continuously variable transmission (CVT) with gear ratio control system, respectively. In contrast, in Hu et al. (2017), the method by adjusting the inertia of a flywheel is demonstrated based a ball-screw mechanism.

In this chapter, the general framework to realize the semi-active inerter will be introduced in detail. The proposed method is a general framework to realize semi-active inerters, which means that although the proposed framework is illustrated based on a ball-screw inerter, other types of semi-active inerters such as rack-pinion inerters and hydraulic inerters can similarly be constructed. Besides, a novel semi-active-inerter-based ATVA (SIATVA) is proposed. Two control frameworks for the SIATVA, that is, the frequency-tracker-based (FT) control and the phase-detector-based (PD) control, are proposed. The proposed control frameworks are also general frameworks in the sense that other frequency-tracking and phase-detection techniques can similarly be implemented.

5.2 Preliminary

The tuned vibration absorber (TVA) is an auxiliary spring-mass system connected to a host structure in order to suppress the vibration of the host structure. It is a classical vibration control device extensively used in many fields of civil and mechanical engineering (Den Hartog 1985). Note that although the TVA has the similar structure with the dynamic vibration absorber (DVA) or tuned mass damper (TMD) (see Chap. 4, they are normally applied in different situations. For the DVA or TMD, the spring-mass system is implemented to suppress the vibration of the host structure over a wide range of excitation frequencies, such as the inerter-based DVAs in Chap. 4; while the TVA is to suppress the vibration at a specific excitation frequency (Bonello 2011; Brennan 2006). Figure 5.1 shows the schematic of TVA, where the principle idea is

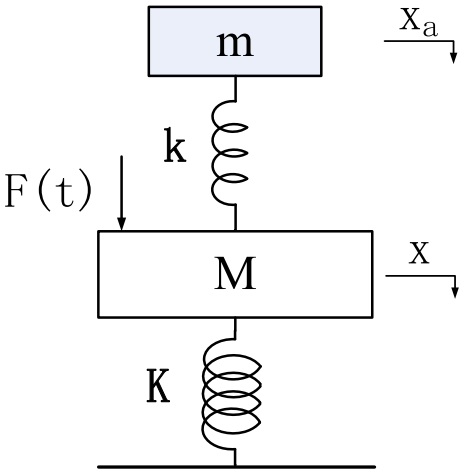

Fig. 5.1 The schematic of tuned vibration absorber (TVA), where K and M denote the host structure, k and m denote the spring-mass system

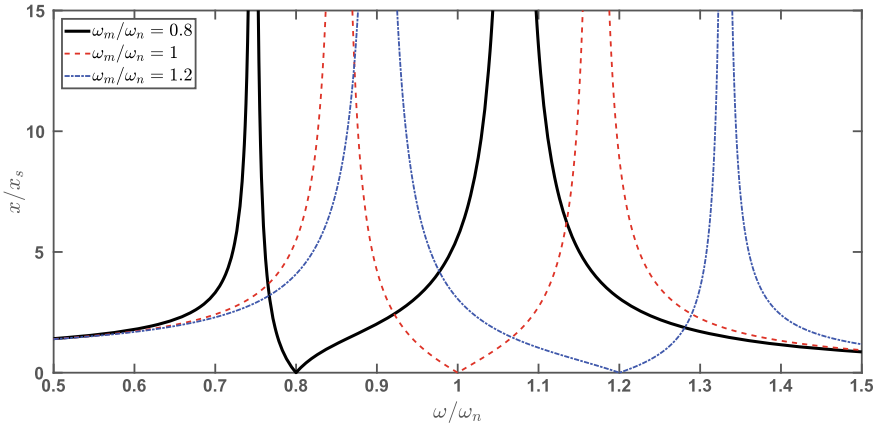

Fig. 5.2 The frequency response of the TVA with different ω_m, where $\omega_m = \sqrt{\frac{k}{m}}$, and $\omega_n = \sqrt{\frac{K}{M}}$

that if the damping of the auxiliary spring-mass system is neglectable, the vibration of the host structure at a specific frequency can be totally absorbed. As shown in Fig. 5.2 with different stiffness-mass pairs, if the stiffness and mass of the TVA are properly tuned, the vibration at a specific frequency can be totally suppressed.

Note that for the TVA, only the vibration at a specific frequency can be suppressed. This may be not applicable in practice as the environmental conditions may vary in time, and if the excitation frequency varies, the TVA would be not effective. To overcome this drawback, the adaptive TVA (ATVA) is developed, where the parameters (stiffness or mass) can be adapted online. A beam-like adjustable-stiffness TVA is

proposed in Brennan (2006), where the stiffness is adjusted by moving the beams apart. Other types of ATVA can be realized by using shape memory alloy (Jayender et al. 2008), piezoceramic elements (Davis and Lesieutre 1999), etc. (see Bonello 2011; Brennan 2006) and references therein). In this chapter, another realization of ATVA by using the proposed semi-active inerter will be introduced and tested.

5.3 Semi-active Inerter

5.3.1 The Existing Inerters

Most of the existing inerters (Smith 2002; Chen et al. 2009; Wang and Su 2008; Wang et al. 2011) utilize a flywheel to realize the "inerter effect", and for all the existing flywheel-based inerters (Smith 2002; Chen et al. 2009; Wang and Su 2008; Wang et al. 2011), the inertance can be represented as the product of the square of a transmission ratio β and the moment of inertia of the flywheel J as follows

$$b = \beta^2 J. \tag{5.1}$$

For example, for the ballscrew inerter (Chen et al. 2009; Wang and Su 2008), β equals $(2\pi/p)$, where p is the pitch of the screw in units of $m/revolution$; for the rack-pinion inerter (Smith 2002; Chen et al. 2009), β is determined by the radiuses of the gears, pinions and the flywheel; for the hydraulic inerter in Wang et al. (2011), β is determined by the area of the piston.

Therefore, two means can be utilized to realize the semi-active inerter: the first one is to adaptively control the transmission ratio β online; the other is to adaptively control the moment of inertia of the flywheel J online. In this study, the latter is concerned and the method by replacing the fixed-inertia flywheel with a controllable-inertia flywheel (CIF) will be described in the following.

5.3.2 The Controllable-Inertia Flywheel (CIF)

In this study, a CIF is proposed based on the moving mechanical masses method (Schumacher 1991). Figure 5.3 shows the schematic of the proposed CIF. It involves at least two moving masses, which can radially move along the slots of the flywheel's main body. The slots are some channels enforcing the moving masses move radially and straightly. The moving masses are engaged with the collar through linkages, where the collar can move along the rotational axis. The position of the moving masses on the main body can be controlled by adjusting the position of the collar. An electric motor is mounted on the support structure to adjust the position of the collar,

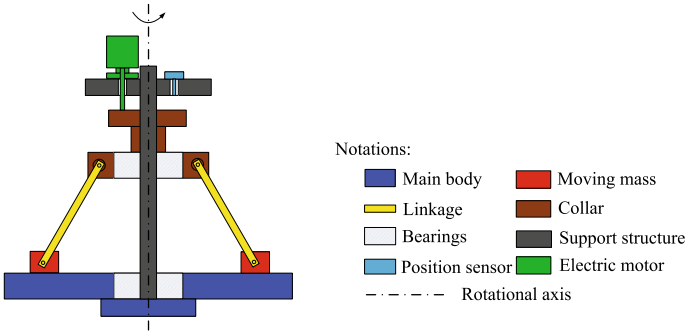

Fig. 5.3 The schematic of the proposed CIF

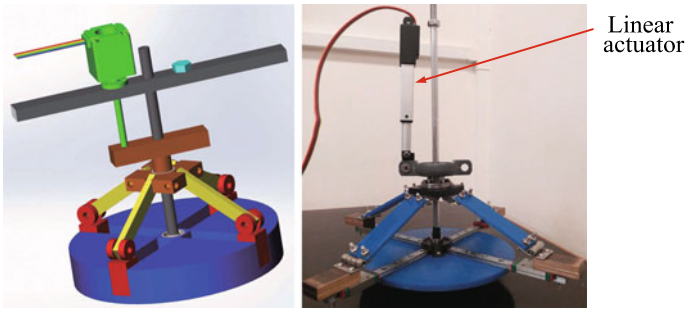

Fig. 5.4 The 3D representation (left) and a prototype (right) of the proposed CIF

and the support structure is fixed and cannot move in any direction. The position sensor is used to measure the distance between the support structure and the collar.

Different from the CIF in Schumacher (1991), in this chapter, two bearings are employed among the collar, the main body of the flywheel, and the support structure, as shown in Fig. 5.3. Thus, during rotation of the flywheel, the upper part of the collar and the support structure do not rotate with the flywheel, guaranteeing the smooth movement of the collar when pushed up and down by the electric motor. Figure 5.4 shows the 3D representation and a prototype of the proposed CIF with four moving masses, where in the prototype, the electrical motor and the position sensor have been embedded in the linear actuator.

Note that the number of moving masses can be adjusted if necessary. The moment of inertia of the CIF can be classified into two parts: the static part and the variable part. The static part includes the main body of the flywheel, the lower part of the collar, and the bearings, whose moment of inertia remains constant during rotation of the CIF. In contrast, the moving masses and the linkages constitute the variable part, whose moment of inertia can be controlled online.

Denote J, J_{static}, and $J_{variable}$ as the moment of inertia of the CIF, the static part, and the variable part, respectively. One has

$$J = J_{static} + J_{variable}, \tag{5.2}$$

where $J_{variable}$ is determined by the displacement of the linear actuator η. In this way, the moment of inertia of the CIF can be effectively controlled by varying the displacement of the linear actuator η.

5.3.3 The CIF-Based Semi-active Inerter

In this study, the proposed framework of realizing semi-active inerter is illustrated based on a ball-screw inerter, as shown in Fig. 5.5. Note that the CIF is located at the end of the screw to facilitate the operation of the CIF, which is different from the existing ball-screw inerters in Chen et al. (2009), Wang and Su (2008).

The inertance of the CIF-based semi-active inerter can be represented as

$$b = b_0 + b_v, \tag{5.3}$$

where b_0 and b_v denote the static and the variable inertance, respectively, and $b_0 = \beta^2 J_{static}$, $b_v = \beta^2 J_{variable}$.

The variable inertance b_v is determined by the displacement of the linear actuator η. Therefore, the inertance of the CIF-based semi-active inerter can be represented as

$$b = \Phi(\eta). \tag{5.4}$$

Note that $\Phi(\eta)$ is an increasing function with respect to η, which means that the minimal and maximal inertances of the CIF are $b_{\min} = \Phi(\eta_{\min})$ and $b_{\max} = \Phi(\eta_{\max})$, where $\eta_{\min}$ and $\eta_{\max}$ are the minimal and maximal η, respectively.

5.3.4 Modeling of the Proposed Semi-active Inerter

The proposed CIF-based semi-active inerter utilizes a linear actuator to adjust the displacement η, and the linear actuator is driven by a driven voltage V. Denoting the displacement η as $G(V)$, the dynamics of the CIF-based semi-active inerter can be

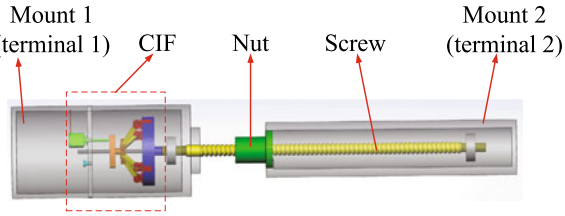

Fig. 5.5 An illustration of the proposed semi-active inerter based on a ballcrew inerter

summarized as

$$F = b\left(\ddot{x}_1 - \ddot{x}_2\right), \tag{5.5}$$

$$b = \Phi(\eta), \tag{5.6}$$

$$\eta = G(V). \tag{5.7}$$

The details on deriving $\Phi(\eta)$ will be introduced in Sect. 5.5.

5.4 Semi-active-Inerter-Based Adaptive Tuned Vibration Absorber

5.4.1 Problem Formulation

Figure 5.6 shows the comparison between the TATVA and the SIATVA, where M, K, C denote the mass, stiffness, and damping coefficient of the primary system, respectively. The object is to reject the harmonic force imposed on the primary mass, where the excitation frequency may vary with time.

Denote F as a sinusoidal force with a time-varying frequency. The transfer function from the disturbing force F to the displacement of the primary system for the SIATVA can be obtained as

$$T = \frac{x}{F} = \frac{bs^2 + k_1}{(Ms^2 + Cs + K)(bs^2 + k_1) + bk_1 s^2}. \tag{5.8}$$

As shown in (5.8), if the SIATVA is tuned to have $\omega = \sqrt{k_1/b}$, where ω is the excitation frequency of the force F, perfect cancellation can be achieved. Perfect cancellation means that the disturbing force F has no influence on the primary mass M. The perfect cancellation condition only involves the parameters of the SIATVA and does not rely on the parameters of the primary system.

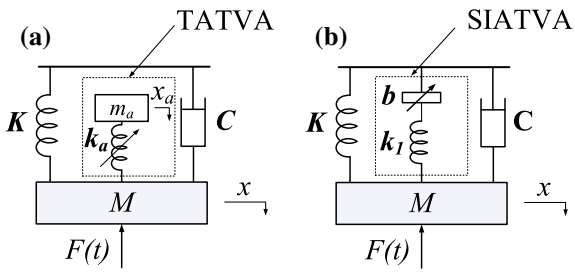

Fig. 5.6 The comparison of the traditional adaptive tuned vibration absorber (TATVA) and the semi-active inerter based adaptive tuned vibration absorber (SIATVA): **a** TATVA; **b** SIATVA

5.4.2 Frequency-Tracker-Based (FT) Control

According to the perfect cancellation condition, for a given stiffness k_1 and a given excitation frequency ω, the required inertance can be obtained as

$$b = \frac{k_1}{\omega^2}. \tag{5.9}$$

Therefore, an intuitive way to control the SIATVA is to track the excitation frequency online, and adjust the inertance according to (5.9). The frequency can be obtained by using a frequency tracker via the measurement of the acceleration of the primary mass. Therefore, only one sensor is required in the FT control.

Various techniques can be employed to track the frequency of harmonic signals online, such as zero-crossing detection (Friedman 1994), Kalman filters (Partovibakhsh and Liu 2014), etc. In this study, a zero-crossing-based frequency tracker is employed for its simplicity and efficiency in the experiments (for the details on zero-crossing detection, see (Friedman 1994) and references therein).

5.4.3 Phase-Detector-Based (PD) Control

Another framework to control the proposed SIATVA system is the phase-detector-based (PD) control. The proposed controller requires two measurements, i.e. the acceleration of the primary mass and the acceleration of the connection point between the spring k_1 and the inerter b.

Denote the displacement of the connection point as y. The transfer function from $\ddot{x}$ to $\ddot{y}$ can be obtained as $\ddot{y}/\ddot{x} = k_1/(k_1 + bs^2)$. Assume the excitation frequency is ω_0, and let $\ddot{x} = a_x \sin(\omega_0 t)$, where a_x is the amplitude, then $\ddot{y}$ can be represented as $\ddot{y} = a_y \sin(\omega_0 t - \phi)$, where $a_y = a_x k_1/(|k_1 - b\omega_0^2|)$, and

$$\phi = \begin{cases} 0 & \text{if } k_1/b > \omega_0^2, \\ \pi & \text{if } k_1/b < \omega_0^2, \\ \pi/2 & \text{if } k_1/b = \omega_0^2. \end{cases}$$

It is clear that the phase difference between $\ddot{x}$ and $\ddot{y}$ is $\pi/2$ when the perfect cancellation occurs. Therefore, the phase difference between ϕ and $\pi/2$ can be employed as the error signal, and a proper controller can be designed to minimize the phase difference. Note that if $\phi > \pi/2$, the inertance b should be decreased, and if $\phi < \pi/2$, the inertance b should be increased. It is also desirable for the designed controller to have large adjustments if the difference is significantly different from 0 and have small adjustments if it is close to 0. Since the inertance is adjusted by the displacement of the linear actuator η, a control law for η can be derived as

$$\eta_k - \eta_{k-1} = P_1\left(\frac{\pi}{2} - \phi_k\right) + P_3\left(\frac{\pi}{2} - \phi_k\right)^3 - D\dot{\phi}_k, \tag{5.10}$$

where k is the sample index, the cubic term is to make the controller have small adjustments if the phase difference is close to 0, and the derivative term is to improve the dynamic response of the system.

The phase angle ϕ can be estimated by the following equation (Brennan 2006)

$$\phi = \cos^{-1}\left(\frac{\frac{1}{T}\int_0^T \ddot{x}\ddot{y}dt}{\ddot{x}_{rms}\ddot{y}_{rms}}\right),$$

where T is the period of signals $\ddot{x}$ and $\ddot{y}$, and $\ddot{x}_{rms}$ and $\ddot{y}_{rms}$ are the root-mean-square (rms) values of the signal $\ddot{x}$ and $\ddot{y}$, respectively. For a sinusoidal signal, its rms value equals $1/\sqrt{2}$ of its magnitude.

5.5 Experimental Evaluation

In this section, the effectiveness of the proposed semi-active inerter and SIATVA will be experimentally verified.

5.5.1 Experimental Platform Description

As shown in Fig. 5.7, the disturbing force $F(t)$ imposed on the primary mass M is induced by the vibration shaker through the intermediate mass and intermediate spring; the sensors 1 and 2 are two accelerometers, where sensor 1 is used to measure the acceleration of the primary mass M, and sensor 2 is used to measure the acceleration of the point between the spring k_1 and the semi-active inerter b; the spring k_1 in Fig. 5.6 is realized by four parallel springs. The proposed FT control and PD control are realized by using SIMULINK. Displacements are obtained from accelerations by performing Fourier transformation and then conducting numerical integration.

The parameters of the experimental platform and the control methods are given in Table 5.1, where the parameters in the FT control and PD control are chosen by using the trail-and-error method. According to the perfect cancellation condition in Sect. 5.4, the effective frequency range for the proposed SIATVA is in $[\omega_{\min},\ \omega_{\max}]$ where

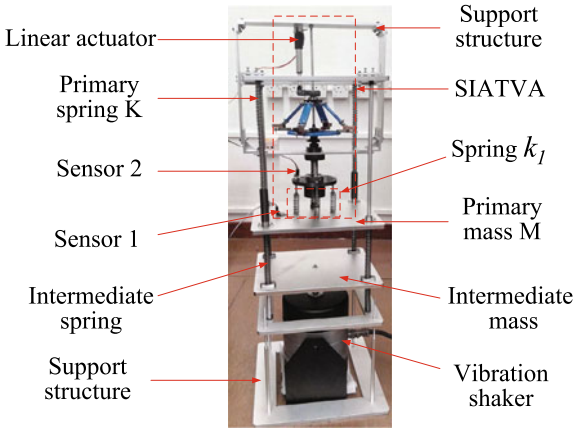

Fig. 5.7 The experimental platform for the proposed SIATVA

$$\omega_{\min} = \sqrt{\frac{k_1}{b_{\max}}} = 6.76 \text{ (rad/s)}, \tag{5.11}$$

$$\omega_{\max} = \sqrt{\frac{k_1}{b_{\min}}} = 12.10 \text{ (rad/s)}. \tag{5.12}$$

Note that compared with the existing ATVAs (Bonello 2011; Brennan 2006), the effective frequency range is quite small due to the limitation of the experimental setup. The approaches to enlarge the effective frequency range can be: enlarging the stiffness k_1, or enlarging the mass of the moving masses, or increasing the number of the moving masses, etc.

As shown in (5.6), the inertance b is determined by the displacement of the linear actuator η. The relation between b and η, i.e. the function $\Phi(\eta)$, can be obtained as follows: from Sect. 5.4, for a given excitation frequency ω, if the inertance satisfies the perfect cancellation condition, the response of the primary mass acceleration will be minimized. Since the spring stiffness k_1 can be measured, one can obtain a relation between b and η by measuring the specific η where minimal acceleration occurs for a given frequency ω, and then obtain b by $b = k_1/\omega^2$.

Figure 5.8 shows the relation between the inertance b and the linear actuator displacement η from both theoretical calculation and experimental measurement, where one sees that the theoretical calculation is consistent with the experimental measurement. The moment of inertia is a quadratic function of the rotary radius, and the rotary radius is a linear function of η. Therefore, a second-order polynomial is employed to fit the measured inertance and η in a least squares sense. The obtained curve fitting equation is

$$b = -0.0494\eta^2 + 6.5257\eta + 124.1974, \tag{5.13}$$

which will be employed as $\Phi(\eta)$ in the experiments in the FT control.

Table 5.1 The parameters of the experimental platform

	Description	Value
The primary system	Primary mass, M	2.5 kg
	Primary spring, K	896 N/m
	The intermediate mass	2.5 kg
	The intermediate spring	3576 N/m
Semi-active inerter	Number of moving masses, n	4
	Mass of per moving mass, m_{mm}	62.60 g
	Mass of the CIF main body, m_m	152.30 g
	Mass of the collar, m_c	60.20 g
	Mass of the bearing, m_b	24.90 g
	Mass of per linkage, m_L	3.9 g
	Pitch of the ball-screw, p	2 cm
	Min. rotary radius of moving masses	21.75 mm
	Max. rotary radius of moving masses	90.70 mm
	Min. linear actuator disp., $\eta_{\min}$	0 mm
	Max. linear actuator disp., $\eta_{\max}$	42 mm
	Static moment of inertia, J_{static}	0.5452 gm^2
	Static inertance from calculation, b_{static}	53.81 kg
	Min. inertance from calculation, $b_{\min}$	99.11 kg
	Max. inertance from calculation, $b_{\max}$	316.72 kg
	Speed of the linear actuator	15 mm/s
Spring k_1	Stiffness, k_1	14.5 kN/m
FT control	Sample time, T_s	10 ms
	Zero-crossing number per evaluation, N	25
PD control	Sample time, T_s	10 ms
	Linear proportional gain, P_1	2.5
	Cubic proportional gain, P_3	20
	Derivative gain, D	6

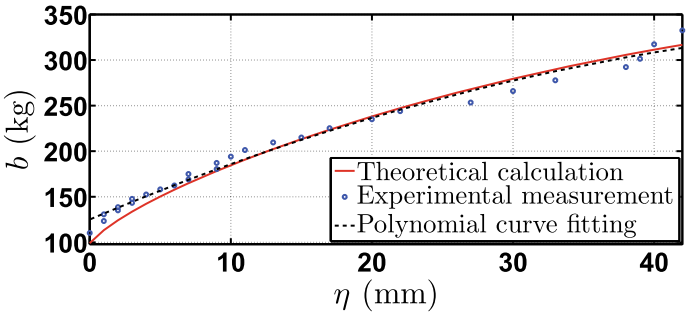

Fig. 5.8 Comparison of the relation between inertance b and linear actuator displacement η via theoretical calculation and experimental measurement

5.5.2 Test Cases

5.5.2.1 Test Case 1

This test is to demonstrate that the proposed SIATVA has the ability to adapt the inertance and thus to handle the excitation frequency variation by using the FT control and PD control. In the experiment, the excitation frequency ω varies as follows:

$$\omega = \begin{cases} 6.90 & t \in [0, 50], \\ 10.11 & t \in (50, 100], \\ 6.85 & t \in (100, 150]. \end{cases}$$

Figures 5.9 and 5.10 show the experimental results. Since some inherent nonlinearities exist in the experimental platform, such as the play in the ball screw, the friction among the components, etc., the perfect acceleration of the primary system cannot be achieved. However, compared with the case without the SIATVA, the proposed SIATVA can still significantly reduce the displacement of the primary mass. As shown in Fig. 5.10, both the FT control and PD control can automatically adjust the linear actuator displacement η to handle the variation of the excitation frequency.

Moreover, the experimental results show that the PD control tends to be more fluctuant than the FT control. The reason for this is that in this chapter, the frequency tracker tracks the frequency more stably than the phase detector detecting the phase, as shown in Fig. 5.10. Through experiments, it is also found that the FT control heavily relies on the performance of the frequency tracker, and if the disturbing force is too noisy (the high-order harmonics are too large), the FT control performs poorly. In this sense, the PD control is more robust to the variation of the disturbance than the FT control. However, all these issues can be alleviated by employing more efficient and more reliable frequency trackers and phase-detector-based controllers, and the main purpose of this test is to show that both of them are effective to control the SIATVA.

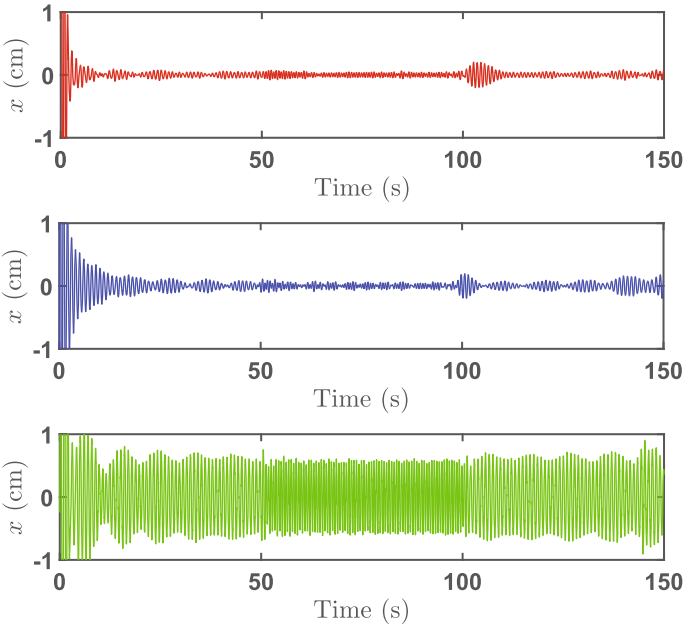

Fig. 5.9 The primary mass displacement in Test case 1: top: FT control; middle: PD control; bottom: without SIATVA

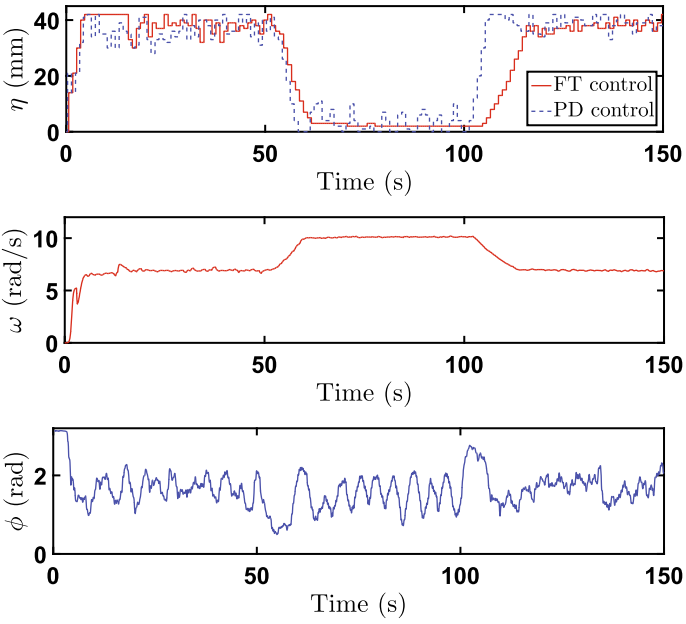

Fig. 5.10 Test case 1: the displacement of the linear actuator (top); the estimated frequency in FT control (middle); the phase difference in PD control (bottom)

5.5.2.2 Test Case 2

This test is to show the ability of the SIATVA to tolerate the variation of the primary system. The excitation frequency ω is 8.19 rad/s. The primary mass experiences a 43.6% sudden change, as represented as follows:

$$M = \begin{cases} 2.5 & t \in [0, 50], \\ 3.59 & t \in (50, 100], \\ 2.5 & t \in (100, 150]. \end{cases}$$

As shown in Fig. 5.11, the variation of the primary mass has a negligible influence on the performance of the SIATVA, which means that the proposed SIATVA can be used in a wide range of systems without resetting the parameters. Theoretically, if the inertance and the spring stiffness k_1 are well tuned, the SIATVA can be used in any primary systems. However, if the disturbing force is relatively much larger than the stiffness k_1, the free terminal of the semi-active inerter will undertake a very large vibration, which may lead to the stroke of the semi-active inerter to the limit.

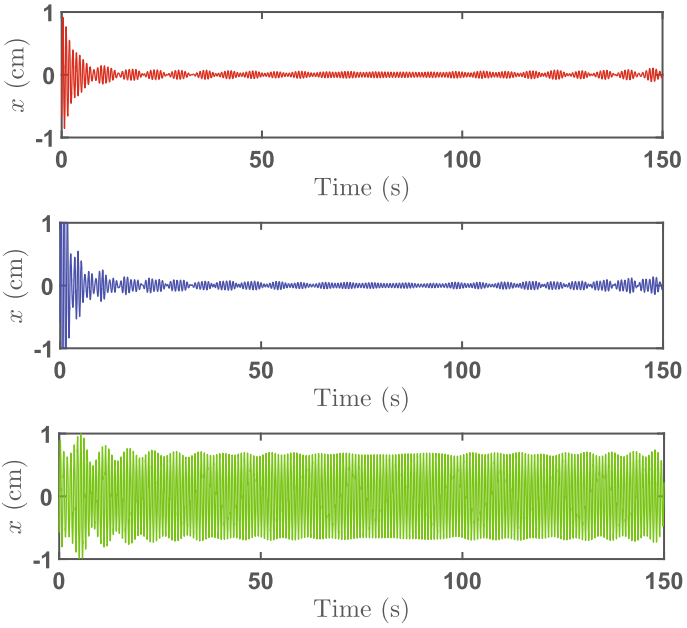

Fig. 5.11 The primary mass displacement in Test case 2: top: FT control; middle: PD control; bottom: without SIATVA

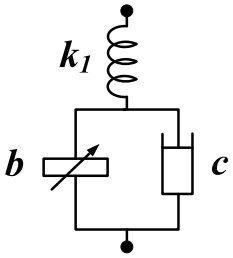

Fig. 5.12 The SIATVA with inherent damping

5.5.3 *The Influence of the Inherent Damping of the Semi-active Inerter*

The physical structure of the semi-active inerter, such as the friction, can introduce some inherent damping to the proposed semi-active inerter. In this study, the inherent damping is modeled as a viscous damper with a damping coefficient c. Then, the SIATVA can be modeled as shown in Fig. 5.12. The transfer function (5.8) can be rewritten as

$$\frac{x}{F} = \frac{bs^2 + cs + k_1}{(Ms^2 + Cs + K)(bs^2 + cs + k_1) + k_1(bs^2 + cs)},$$

where one sees that perfect cancellation cannot be achieved for a nonzero c. Figure 5.13 shows the frequency response of the primary mass's displacement with respect to different values of the inherent damping c, where the inertance b is set to be 200 kg. It is shown in Fig. 5.13 that the larger the inherent damping is, the worse the performance of the SIATVA will be, as increasing the inherent damping enlarges the displacement of the primary mass around the perfect cancellation frequency.

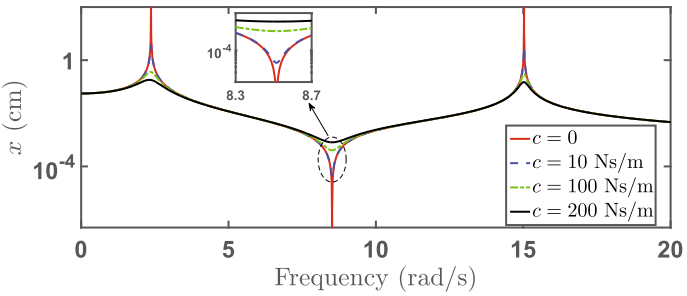

Fig. 5.13 The frequency response of the primary mass displacement with respect to different inerter inherent damping

5.6 Conclusions

In this chapter, a novel framework to realize the semi-active inerter and a novel semi-active-inerter-based adaptive tuneable vibration absorber (SIATVA) have been proposed. The proposed semi-active inerter can be obtained by replacing the fixed-inertia flywheel in the flywheel-based inerters with a controllable-inertia flywheel (CIF). Two frameworks to control the proposed SIATVA have been presented by using the frequency information (FT control) and the phase information (PD control), separately. Experimental results demonstrated that the proposed SIATVA with both the FT control and the PD control can effectively neutralize the vibration of the primary mass. The proposed SIATVA can also tolerate the parameter variation of the primary system, and can be applied to a variety of primary systems without resetting the parameters of the SIATVA. The fact that the inherent damping can degrade the performance of the SIATVA system was also demonstrated.

In terms of these two control methods, the FT control requires only one sensor while the PD control demands two. It was also found in the experiments that the FT control heavily relied on the performance of the frequency tracker, and the PD control was more fluctuant than the FT control. Therefore, it depends on the real applications to determine which method is more suitable in practice, and the main purpose of this chapter is just to show the effectiveness of these two methods in controlling the proposed SIATVA.

References

Bonello, P. (2011). Adaptive tuned vibration absorbers: Design principles. In F. Beltran-Carbajal (Ed.), *concepts and physical implementation, in Vibration Analysis and Control-New Trends and Developments* (pp. 1–26). Croatia: InTech.

Brennan, M. J. (2006). Some recent developments in adaptive tuned vibration absorbers/neutralisers. *Shock and Vibration*, *13*, 531–543.

Brzeski, P., Kapitaniak, T., & Perlikowski, P. (2015). Novel type of tuned mass damper with inerter which enables changes of inertance. *Journal of Sound and Vibration*, *349*(2015), 56–66.

Chen, M. Z. Q., Papageorgiou, C., Scheibe, F., Wang, F. C., & Smith, M. C. (2009). The missing mechanical circuit element. *IEEE Circuits and Systems Magazine*, *9*(1), 10–26.

Chen, M. Z. Q., Hu, Y., Li, C., & Chen, G. (2014). *Semi-active suspension with semi-active inerter and semi-active damper, Proceedings of the 19th IFAC World Congress* (pp. 11225–11230). South Africa: Cape Town.

Davis, C., & Lesieutre, G. A. (1999). An actively tuned solid-state vibration absorber using capacitive shunting of piezoelectric stiffness. *Journal of Sound and Vibration*, *232*(3), 601–617.

Den Hartog, J. P. (1985). *Mechanical vibrations*. New York, USA: Dover Publications Inc.

Friedman, V. (1994). A zero crossing algorithm for the estimation of the frequency of a single sinusoid in white noise. *IEEE Transactions on Signal Processing*, *42*(6), 1565–1569.

Gartner, B. J., & Smith, M. C. (2011). Damper and inertial hydraulic device, U.S. Patent 13/577, 234.

Hu, Y., Chen, M. Z. Q, Xu, S., & Liu, Y. (2017). Semiactive inerter and its application in adaptive tuned vibration absorbers. *IEEE Transactions on Control Systems Technology*, *25*(1), 294–300.

Jayender, J., Patel, R. V., Nikumb, S., & Ostojic, M. (2008). Modeling and control of shape memory alloy actuators. *IEEE Transactions on Control Systems Technology*, *16*(2), 279–287.

Li, P., Lam, J., & Cheung, K.-C. (2014). Investigation on semi-active control of vehicle suspension using adaptive inerter. *The 21st International Congress on Sound and Vibration*, 13–17 July 204, Beijing, China.

Li, P., Lam, J., & Cheung, K.-C. (2015). Control of vehicle suspension using an adaptive inerter. *Proceedings of the Institution of Mechanical Engineers, Part D: Journal of Automobile Engineering*, *229*(14), 1934–1943.

Partovibakhsh, M., & Liu, G. (2014). An adaptive Unscented Kalman Filtering approach for online estimation of model parameters and state-of-charge of lithium-ion batteries for autonomous mobile robots. *IEEE Transactions on Control Systems Technology*, *23*(1), 357–363.

Smith, M. C. (2002). Synthesis of mechanical networks: The inerter. *IEEE Transactions on Automatic Control*, *47*(1), 1648–1662.

Schumacher, L. L. (1991). Controllable inertia flywheel, U.S. Patent 4,995,282.

Tuluie, R. (2010). Fluid Inerter, U.S. Patent 13/575, 017.

Tsai, M.-C., & Huang, C.-C. (2011). Development of a variable-inertia device with a magnetic planetary Ggearbox. *IEEE/ASME Transactions on Mechatronics*, *16*(6), 1120–1128.

Wang, F.-C., & Su, W.-J. (2008). Impact of inerter nonlinearities on vehicle suspension control. *Vehicle System Dynamics*, *46*(7), 575–595.

Wang, F.-C., Hong, M. F., & Lin, T. C. (2011). Designing and testing a hydraulic inerter. *Proceedings of the Institution of Mechanical Engineers, Part C: Journal of Mechanical Engineering Science*, *225*(1), 66–72.

Zhang, X., Ahmadian, M., & Guo, K. (2010). A comparison of a semi-active inerter and a semi-active suspension. *SAE Technical Paper*, 2010-01-1903, https://doi.org/10.4271/2010-01-1903.